ANALYTICAL FRAMEWORK FOR THE ELECTRIFICATION OF LIGHT ROTORCRAFT FOR URBAN AIR MOBILITY

Francesco Mazzeo, francesco.mazzeo@unimore.it, University of Modena and Reggio Emilia (Italy)

Emanuele L. de Angelis, emanuele.deangelis4@unibo.it, University of Bologna (Italy)

Fabrizio Giulietti, fabrizio.giulietti@unibo.it, University of Bologna (Italy)

Francesco Leali, francesco.leali@unimore.it, University of Modena and Reggio Emilia (Italy)

Alessandro Talamelli, alessandro.talamelli@unibo.it, University of Bologna (Italy)

Abstract

The present paper develops an analytical methodology to design electrical powertrains and to study the performance of multirotor configurations. The model is based on the general momentum and blade element theories and it has been modified to take into account for multiple rotors and vertical flight conditions. An iterative procedure to design battery packs and compute the discharge time is provided. The original contribution of the article is represented by the application of the above-mentioned methodology to design and compare different eVTOL vehicles against a reference lightweight helicopter with specified design features. As a result, a quadrotor configuration is identified as the best solution to fulfill all the mission requirements and improve the performance of the helicopter with additional benefits.

Keywords

eVTOL, helicopter, multirotor, side-by-side, performance analysis, battery design, mission design

1. INTRODUCTION

The term “Urban Air Mobility” (UAM) defines an advanced air transportation system for passengers and cargo, in and around densely populated areas and urban environments [1]. In order to operate in these restricted regions and to be considered part of a UAM ecosystem, aerial vehicles must respect two fundamental requirements: vertical take-off and landing (VTOL) capabilities and sustainability. Electric and hybrid VTOLs have been developed in order to satisfy mission requirements for range, endurance and speed [2]. The use of these vehicles for public transport would represent an outstanding revolution of the urban transport sector in modern societies. Considerable reduction of local CO_2 emissions and traffic congestions in large cities would be a couple of important objectives achievable by moving part of the “transport network” on air. A UAM ecosystem would guarantee a much faster and safer mobility: the interconnection between the vehicles would lower the risk of fatal accidents and ease the fleet management, while the direct routes would provide up to 70% of time saved on average on a standard city travel time [3]. Most of the recent research efforts are focused on the design of innovative eVTOL configurations, suitable for different goals. Johnson *et al.* [4] presented a performance study of three concept vehicles for air taxi operations: a single-passenger electric quadrotor, a six-passenger side-by-side helicopter with hybrid propulsion and a fifteen-passenger tiltwing with turbo-electric propulsion. In their analysis, the concept vehicles were compared considering the ideal mission requirements for each of them. As expected, the quadrotor resulted to be the best configuration for short range missions in urban environment because of its capacity of operating in restricted areas despite of a limited endurance. The hybrid-powered side-by-side helicopter guaranteed optimal performance in medium range missions, while to maximize the range a turbo-electric propulsion system is still needed. In the latter case, the tilt-wing solution provides much higher efficiency in cruise than the other configurations. In order to reduce the local CO_2 emissions, sustainable propulsion systems must be exploited. Zong *et al.* [2] studied the potential of electric and hybrid propulsion systems on small VTOL UAVs (Unmanned Aerial Vehicles) summarizing the advantages of series/parallel hybrid configurations and the performance on designed mission profiles. With the current level of battery technology, the all-electric setup has very limited endurance and range, which is why eVTOLs are still not very much employed. There are many examples of innovative prototypes with electric propulsion systems that are still under certification processes: the 4-seater multirotor CityAirbus [5] and the vectored thrust 5-seater Joby S4 [6] are two eVTOLs with promising performance developed by AIRBUS and NASA. According to the design

specifications shared by the producers, Bacchini and Cestino [7] conducted an analytical study on the endurance and speed of commercial eVTOLs. In the analysis, they computed the mission performance of the coaxial multirotor E-Hang 184 [8], the lift+cruise Kitty Hawk Cora and the vectored thrust Lilium Jet [9], confirming that the multirotor represents the best solution in hovering conditions, while a vectored thrust guarantees higher range and speed. The lift + cruise represents a compromise between hovering capabilities and cruise, and it can be considered as optimal for mixed, medium range missions. However, none of the above-mentioned studies investigated the capabilities of different all-electric VTOLs compared to classical configurations, leaving an important research gap in that sector. The aim of the present paper is to fill in this gap by providing a methodology for the electrification of a 600 kg lightweight helicopter, along with the presentation of an analytical versatile framework for the study of the performance of general eVTOLs. Three different multirotor designs are developed to fulfill the requirements of a reference mission and then compared, together with the helicopter, in order to find the optimal solution to complete the flight. The same unique methodology is applied in all the cases, making the results reliable and comparable.

2. MATHEMATICAL MODELING

2.1. Performance analysis

An overview of the main equations and assumptions to compute the performance of the rotorcraft is here given. The analytical model was described by Avanzini *et al.* [10], and is based on the general momentum and blade element theories. It has been modified to take into account for multiple rotors and vertical flight conditions, by neglecting the aerodynamic interactions between the rotors and assuming each of them working separately. The total power required by the shaft of the eVTOL in steady flight is thus computed by means of the power balance equation as

$$P_{sh} = (P_p + N_{mr}P_{mr})/\eta_{mr} + P_{tr}/\eta_{tr} + P_s \quad (1)$$

where P_p is the parasite power due to fuselage drag, N_r is the number of main rotors, η_{mr} and η_{tr} are the main and tail rotor transmission efficiencies (assumed to be constant) and P_s is the power required by the auxiliary systems (assumed to be constant). P_{mr} and P_{tr} represent the power required by the main/tail rotor and their computation is reported by Avanzini [10]. The main modification of their model, consists in splitting the thrust required to sustain the rotorcraft into N_r different contributions, in order to separately estimate the performance of each rotor. T_i is the thrust provided by a single main rotor and can be computed as

$$T_i = \sqrt{\left(\frac{W}{N_r}\right)^2 + \left(\frac{D}{N_r}\right)^2} \quad (2)$$

where W is the total weight and D is the fuselage drag computed by using an equivalent flat plate parasitic area f, thus $D = 0.5\rho f U^2$ (U is the true airspeed).

For vertical flight condition, the model is modified to take into account for the incoming vertical flow occurring in steady climbing and descending conditions. In particular, the parasitic power is computed as

$$P_p = D_V|U_V| = (0.5\rho f_V U_V^2)|U_V| \quad (3)$$

where U_V is the climbing/descending speed and f_V is the equivalent parasitic flat plate area in the vertical direction. For sake of simplicity, the contribution of the induced speed v_i to the vertical drag has been neglected. The air density ρ is assumed to be the average value between the initial and final altitude of the steady vertical motion. The induced power P_{ind} has been also modified for vertical flight, as the induced velocity v_i has to take into account for the vertical speed. In particular, the semi-analytical model developed by Johnson [11] is used to estimate the induced speed within wake, vortex and windmill brake regions for both climbing and descending. The final expression for the power is

$$P_{ind} = k_{ind}T_i(U_V + v_i)\ . \quad (4)$$

The factor k_{ind} is the induced power factor and it is the ratio between the induced and ideal power defined by the momentum theory. The factor takes into account for several aerodynamic losses such as the blade tip losses and non-uniformity of the inflow. Mostafa *et al.* [7,8] conducted an experimental study to estimate that factor in different insects' wings, proving its dependency with the number of blades, linear twist and thrust coefficient. However, for sake of simplicity and because of the lack of experimental data for rotorcraft, k_{ind} is kept constant in this analysis and set equal to 1.25.

2.2. Configuration design methodology

The main goal of this paper is to design and compare different configurations of eVTOL according to an objective mission. Three different preliminary design are produced by starting from a reference vehicle. In particular, a turbine-powered lightweight rotorcraft with maximum take-off mass equal to 600 kg is selected as starting design. The

vehicle is ideally electrified by removing all the components related to the turbine engine and by replacing them with an electrical motor and a battery. Data of the helicopter can be found in Appendix A. The design methodology [14] consists in taking the same fuselage and structure of the reference design and replace the main rotor with a certain number of smaller ones in order to satisfy the requirements in Table 1

Requirement	Value
• Maximum $MTOW$	600 kg
• Maximum width L	7.6 m
• Minimum payload	175 kg (2 pax.)
• Discharge limit (SOC)	20 %
• Max. hov. throttle at 500 m	65 %
• Objective endurance	50 min

Table 1: Design specifications

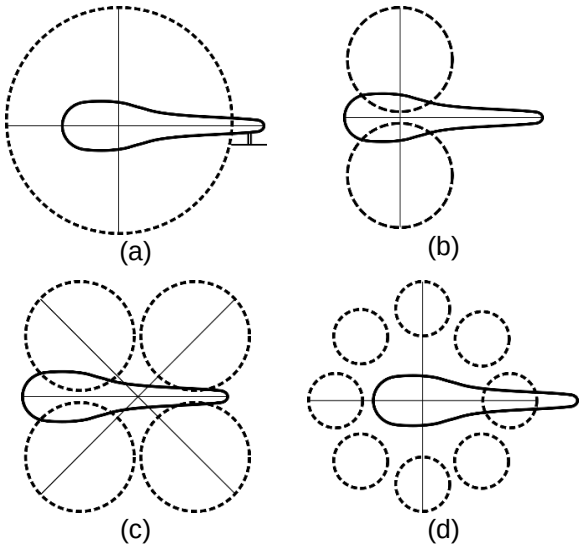

Figure 1: Configurations design. (a) Helicopter (b) Side-by-side (c) Quadrotor (d) Octarotor

A side-by-side helicopter, a quadrotor and an octarotor design are investigated (Figure 1). Because of the lack of a well sized motor, the hexarotor configuration has not been explored. Employing the same fuselage design guarantees that the different eVTOLs have enough space to carry at least the same payload of the reference helicopter. The same value of equivalent flat plate parasitic area can be also used to estimate its drag. The blade design is also similar: blade linear twist and aspect ratio remain unchanged, as well as the aerodynamic drag coefficient and the transmission efficiency η_{mr}. To estimate the weight of the single blade, the following assumption, based on a scaling law, is considered:

$$m_{bl}^{i} = \frac{m_{bl}^{0}}{R_0} R_i \tag{5}$$

where m_{bl}^{i}, m_{bl}^{0}, R_i and R_0 are respectively the mass and the radius of the designed and the reference eVTOL. The number of blades is chosen according to the best performance, i.e. 2 blades in the helicopter, quadrotor and octarotor and 3 blades in the side-by-side design. Finally, an important remark must be stated about the rotational frequency Ω of the rotors. One of the main differences between helicopters and multirotor is the fact that the formers operate at constant Ω and variable collective pitch, while the latter usually operate at variable Ω and the blade pitch remains unchanged. In order to be able to apply the same design methodology for all the configurations, a constant Ω approach is selected. The sizing of this parameter, strictly connected to the tip speed, is not straightforward and depends on several limitations such as stall angle of attack, noise considerations, power and torque demand and autorotation performance [15]. In this analysis, the tip speed is selected in agreement with the design produced by Johnson [4] for side-by-side helicopters and multirotors (see Appendix A).

2.3. Battery design

One of the most challenging issues of this study is the battery pack design methodology. A known cell type is used to build a complete battery pack that is compatible with the chosen electrical motor and respect the limits for maximum take-off weight ($MTOW$).

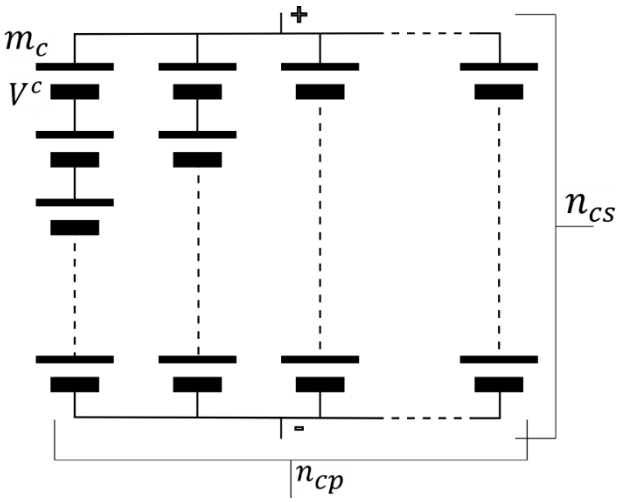

Figure 2: Battery pack configuration

The battery is made of a set of single cells arranged in series and parallel in order to maximize the

overall capacity and match with the voltage of the motor in the hovering condition (Figure 2). The design methodology requires an iterative procedure, because every time a series of cells is added, the overall $MTOW$ changes according to the increment of battery mass. When this happens, the power required to hover is modified and the electrical motor has to operate at a different voltage condition. It is worth mentioning that, by arranging a set of cells in series, the overall voltage obtained for the battery pack is the sum of the single voltages of the cells. On the other hand, by arranging a set of cells in parallel, the voltage remains unchanged, but the overall capacity becomes the sum of the capacities of each series of cells. In this way, the nominal voltage required can be achieved by arranging cells in series, and the capacity can be maximized by adding series of cells in parallel. An explicative summary of the approach is provided in Figure 3.

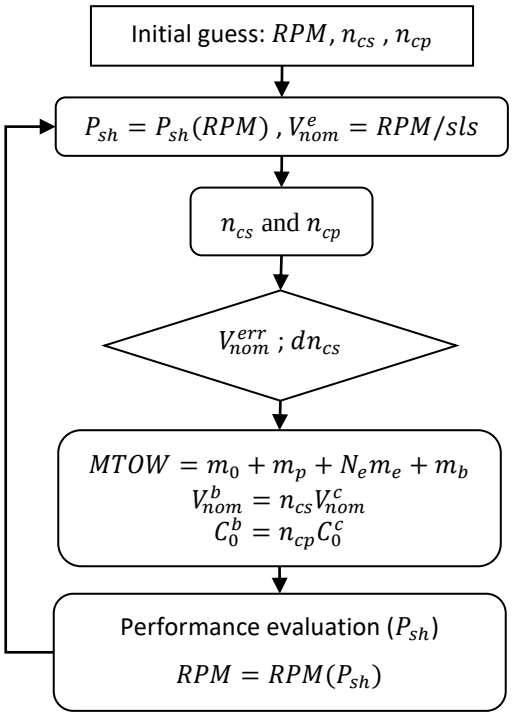

Figure 3: Battery design iterative procedure

The methodology aims to find the suitable combination of n_{cs} and n_{cp} that matches the nominal voltage of the battery V_{nom}^{b} with the nominal voltage of the motor V_{nom}^{e} necessary to keep the rotorcraft in hovering. The power required at the shaft P_{sh} and the rotational frequency of the motor RPM are linked by the characteristic power curve of the electric machine. The specific load speed sls is a parameter of the electrical motor that connects voltage and frequency. At each iteration, the number of cells in series and parallel is computed as

$$n_{cs} = round\left(\frac{V_{nom}^{e}}{V_{nom}^{c}}\right) \quad (6)$$

$$n_{cp}^{new} = n_{cp}^{old} + floor\left(\frac{MTOW_{max} - MTOW(n_{cs}^{new}, n_{cp}^{old})}{m_{serie}}\right) \quad (7)$$

where $MTOW_{max}$ is the maximum allowed total weight, $m_{serie} = n_{cs} m_c$ is the weight of a single series of cells having m_c mass and $MTOW(n_{cs}^{new}, n_{cp}^{old})$ is the total mass computed with a battery having the new n_{cs} and the old n_{cp}. In this way, the n_{cs} tends to match the nominal voltages, while the n_{cp} is used to fill in the remaining available mass and maximize the capacity by adding series of cells in parallel. As a matter of fact, the endurance in ideal discharge conditions is

$$t_{id} = \frac{C_0 V_{nom}}{P_{sh}} \eta_e \ , \quad (8)$$

meaning that for a fixed voltage required, the endurance of the battery can be increased by maximizing its capacity (η_e is the electrical efficiency of the system). Once the new number of cells is computed, the mass of the rotorcraft can be updated by summing up the "empty mass" m_0, the mass occupied by the motors $N_e m_e$ (where N_e and m_e are respectively the number and mass of the single motors), the mass of the battery m_b and the payload m_p. In particular m_0 is defined as the mass of the rotorcraft without the payload and the electric propulsion system, thus battery and motor. The mass of the battery is computed as

$$m_b = n_{cs} n_{cp} m_c \quad (9)$$

Nominal voltage and capacity of the battery are updated as well. Finally, the performances of the vehicle are computed with the new mass, by applying the model described in section 2 and the new power used to restart the new iteration. The algorithm stops when both the requirements on voltage error and number of series cells variation are achieved. Indeed, the stopping criteria are

$$V_{nom}^{err} = \frac{|V_{nom}^{e} - V_{nom}^{b}|}{V_{nom}^{e}} < tolerance \quad (10)$$

and

$$dn_{cs} = n_{cs}^{new} - n_{cs}^{old} = 0 \quad (11)$$

being $\boldsymbol{n_{cs}}$ a discrete parameter.

For the sake of this paper, the Lithium Sulfur (Li-S) cells produced by OXiS [16] are chosen, as they provide a higher energy density than classical Lithium Ion (Li-Ion). For the electrical motor, the series of products provided by EMRAX are employed, because they provide affordable solutions for different power requirements and the

design of their motors is suitable to be located in a light rotorcraft. Details of battery cells are reported in Table 2, while electrical motor parameters can be found in the EMRAX webpage [17].

Battery type: High Energy OXiS Li-S

Voltage range	$V^c_{\min} \div V^c_{max}$	1.9 ÷ 2.6 V
Nominal voltage	V^c_{nom}	2.1 V
Nominal capacity	C^c_0	14.7 Ah
Max. discharge rate	C_{rate}	2 C
Energy density	E_d	400 Wh/kg
Cell mass	m_c	85 ± 2 g

Table 2: Battery cell parametres

2.3.1 Battery discharge model

The development of a reliable constant-power battery discharge model is a fundamental part of the analysis. For the sake of this paper, the results of the experimental study conducted by Avanzini *et al.* [18] are used to extrapolate an analytical framework to estimate the endurance of batteries made of a variable number of Li-S cells. In their analysis they performed a set of experiments on Li-Po batteries to measure the total duration t as a function of the capacity C, the number of cells N and the constant discharge power P_b. An exponential model is chosen to compute this time as

$$t = \alpha(N, P_b) C^{\beta} \tag{12}$$

where α is a function of the power and the number of cells. The experiments retrieved a set of values of α for different P_b and N that were interpolated by applying a variable separation method. Nevertheless, the interpolation used by Avanzini diverges when the number of cells increases and it cannot be applied for the cases considered in this paper. To overcome this issue, a new interpolation method is applied and

$$\alpha(N, P_b) = a(N) P_b^{b(N)} + c(N)\ , \tag{13}$$

where

$$\begin{cases} a(N) = 4.129 \cdot N - 0.2241 \\ b(N) = -1.003 \\ c(N) = -0.03244 \cdot N^{-1.43} + 3.161 \cdot 10^{-4} \end{cases} \tag{14}$$

so $b(N)$ is a constant value and $a(N)$ and $c(N)$ are respectively a linear and an exponential function of N. It is worth mentioning that in order to apply their results to the Li-S batteries employed in this paper, a simple linear proportion is performed by means of the nominal voltage of the cells, thus multiplying the experimental α by $V^c_{nom}(LiS)/V^c_{nom}(LiPo)$.

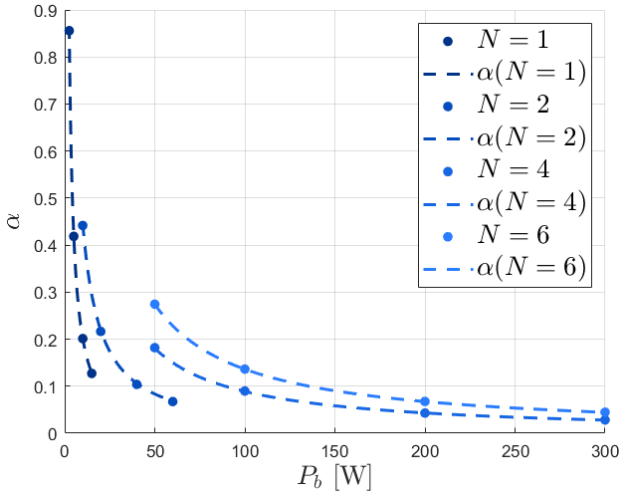

Figure 4: Experimental results and interpolation of α

By applying the described model, developed by Avanzini and then modified to extrapolate data for the present paper, the discharge time of a battery pack can be analytically estimated by knowing its power loading and state of charge.

2.4. Mission design

The aircrafts are designed by following the methodology in section 2.2 and complete a reference mission described in Table 3 .

	Altitude	Speed	Time
Climb	$0 \rightarrow 500\ m$	$U_V = 4\ m/s$	$2.08'$
Hover	$500\ m$	-	$2.00'$
Cruise	$500\ m$	U_{bse}/U_{bsr}	t_c
Hover	$500\ m$	-	$2.00'$
Descent	$500 \rightarrow 0\ m$	$U_V = -4\ m/s$	$2.08'$

Table 3: Mission design

The total duration of the mission is T_{bse} in the best specific endurance condition and T_{bsr} for the best specific range. The cruising time t_c is maximized in order to complete the mission without falling below the discharge limit (section 2.2). As a general rule of thumb, usual batteries cannot be discharged below a certain limit without being damaged. For this reason, a fixed minimum SOC of 20% is set.

3. RESULTS AND DISCUSSION

Together with the electrification of the light helicopter, taken as reference vehicle, three different eVTOL configurations are designed for comparison in this study: a side – by – side (SbS) helicopter, a quadrotor (Quad) and an octarotor (Octa). The aim is to compare the different design with the same type of propulsion system (electric motor) and find the best solution in order to complete the mission reported in section 2.4, while fulfilling the requirements in section 2.2. Therefore, before studying the performance in terms of power, endurance and range, the battery is designed according to the above-mentioned methodology. The results are reported in Table 4.

	$n_{cs} \times n_{cp}$	m_b [kg]	m_e [kg]
Helicopter	222 x 9	169.8	59.5
Sidebyside	129 x 14	153.5	76.9
Quadrotor	73 x 26	161.3	62.4
Octarotor	46 x 26	108.3	108.8

Table 4: Battery designs

The number of cells arranged in series determines the nominal voltage of the battery. As expected, this number decreases inversely with the number of rotors because the single motor needs to provide a smaller power, thus smaller voltage. Being the power required by the single rotor smaller, the remaining empty mass can be filled with parallel series that increase the capacity of the battery and its weight. It is noticeable that the battery weight remains around 160 kg for the first three configurations, while a smaller battery design is achievable in the octarotor. The reason why the last design is much smaller than the others is attributable to the higher mass occupied by the motors. The main problem of the octarotor design, which will be reflected also on its performance, is the oversize of the EMRAX188MV/C. They are the smallest motors produced by EMRAX, but still oversized for the single rotor power requirements. In addition, the octarotor design is itself a high-power demanding configuration, as can be observed in Figure 5. It is noticeable in this graph that the octarotor and side – by – side curves are almost superimposed, because of the similar disc loading.

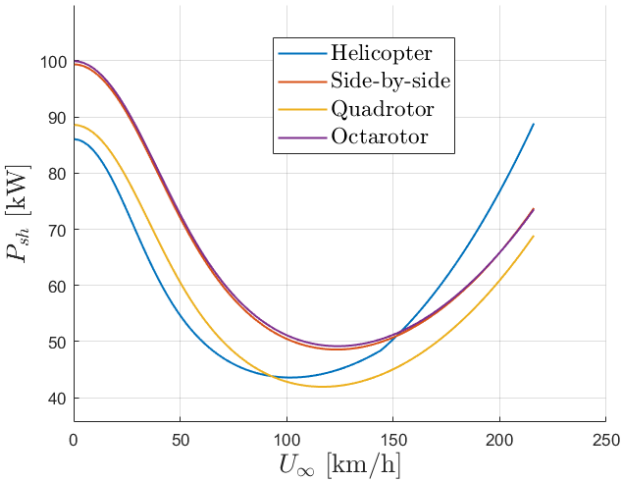

Figure 5: Power curves

While the side – by – side and the octarotor design are the most power demanding at velocities lower than the minimum power speed, above that value the situation changes and the helicopter presents a steeper curve that rapidly increases the power demand at higher speed. This is because of the higher level of profile power reached by the helicopter blades, which are longer and operates at higher tip speed, thus compressibility problems occur. It can be concluded that the helicopter configuration is the less power demanding only at velocities lower than the minimum power condition, while it is not suitable to operate at high cruising speed.

The estimated profiles of the State Of Charge of the battery (SOC) and throttle configurations during the mission are plotted in figures Figure 6 and Figure 7. These figures are referred to the helicopter case, and are showed as an example of the trend of these parameters.

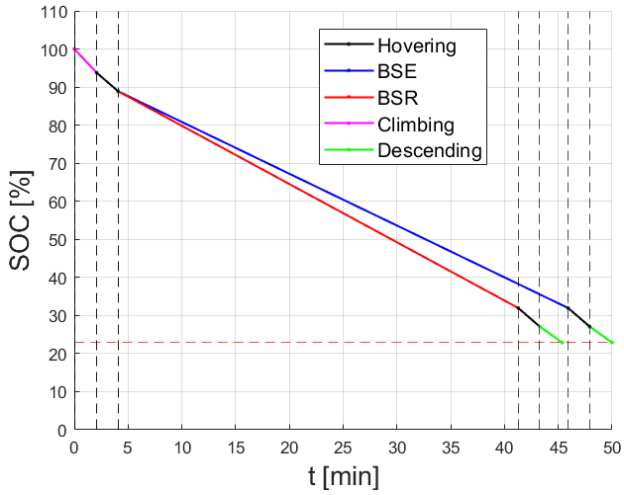

Figure 6: Reference mission State Of Charge (SOC)

The SOC of the fully charged battery constantly decreases with a quasi-linear trend during the different phase of the mission. The higher is the power demand and the higher will be the rate of discharge, thus a steeper slope in that range. It is worth mentioning that the constant – power discharge model (section 2.3.1) provides an approximate rate of discharge which is not perfectly linear, and is more conservative than the typical ideal model.

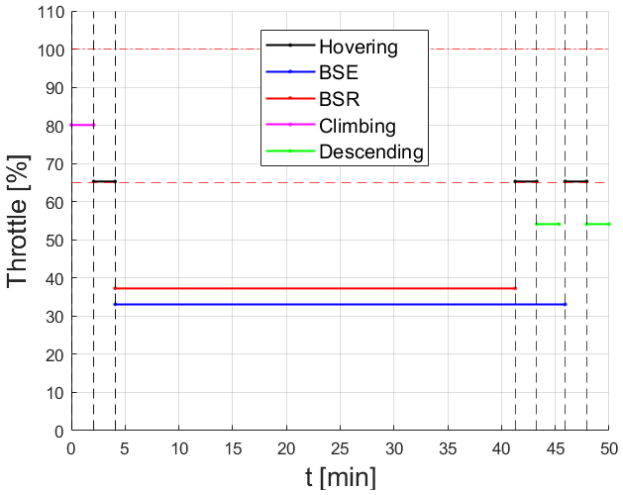

Figure 7: reference mission Throttle profile

The throttle profile gives an idea of the available power of the motors and the capabilities of the eVTOL. The red dashed lines indicate the maximum power (throttle = 100%) and the hovering power limit set in the requirements (throttle = 65%). Cruising at the best specific endurance/range speed is less power demanding than the hovering condition, thus a smaller throttle level is needed. The throttle profiles for the different configurations are reported in Table 5.

%	Climb	Hover	Descent	Cruise *(BSE / BSR)*
Heli	80	65	54	33 / 37
SbS	59	50	43	25 / 30
Quad	73	61	51	29 / 35
Octa	56	48	41	24 / 28

Table 5: Throttle profiles

A proper sizing of the motor and its matching with the eVTOL design is fundamental to achieve optimal performance. For the sake of this paper, the different motors produced by EMRAX are coupled with the configurations. Nevertheless, not all the available solutions are optimal for the specific cases and it turns out that some design are oversized. This is the case of the side-by-side and the octarotor, which have large available power but are unable to complete the 50 min mission.

		Heli	SbS	Quad	Octa
N_r	-	1	2	4	8
$MTOW$	[kg]	588.4	600.0	595.3	598.4
$L\ (R)$	[m]	7.6 (3.8)	7.6 (1.9)	6.0 (1.5)	7.6 (0.95)
DL	[kg/m^2]	13.0	26.5	21.1	26.4
T_{bse}	[min]	50.0	40.6	50.0	26.6
X_{bsr}	[km]	90.7	81.8	100.4	47.1
Res	[%]	2.3	0	0	0

Table 6: Performance results

Table 6 summarizes the main design features of the different configurations and their performance in the reference mission. The helicopter is able to complete the mission with a 2.3% of additional battery charge. In order to maximize the endurance, the side – by – side and octarotor have to reach the maximum width allowed, making these configurations not suitable for this kind of mission. On the other hand, the quadrotor configuration turns out to be the best solution to complete the flight. The EMRAX208MV/CC mounted on this configuration are optimally sized and allows to complete the mission with an "excess of performance". This benefit can be translated into different solutions, depending on the need of the users. For the sake of this paper, the overall width of the eVTOL is reduced of 1.6 m with respect to the other configurations, in order to have a smaller vehicle, suitable to operate in urban environments and restricted areas. However, by allowing a total dimension equal to the other eVTOLs, the endurance can be increased and the mission can be completed with a final additional reserve of 11.41% of the available battery capacity. By fixing the maximum discharge at the limit value as well, the "excess of performance" can be translated into an additional payload of approximately 26 kg.

A final consideration on the four design can be stated. The electrified light rotorcraft in helicopter configuration is able to complete the mission within the range of requirements set, but a limited available power does not allow to achieve high speed or climbing capabilities. The side – by – side design is very high-power demanding and is not able to complete the 50 min mission. Nevertheless, the large battery design allows at least 40 min of endurance with large available power for climbing and high-speed cruising. The high-power demands

of the octarotor, coupled with the bad sizing of the motors, make this configuration the worst in terms of endurance and range. Finally, the quadrotor is turned out to be the best solution for the reference mission because it fulfills all the requirements and provides an additional benefit that can be translated into a larger reserve, payload or a decrease of the overall size.

4. CONCLUSIONS

The present analysis provides an analytical framework for the electrification of light rotorcraft, including a design methodology for multirotor and alternative configurations. The starting point of the study is the electrification of a turbine-powered lightweight helicopter with maximum take-off mass equal to 600 kg, cleared of all the components related to the turbine powertrain (engine, fuel, tanks, additional components). A battery design methodology is presented: a suitable electrical motor is selected and coupled with a battery pack made of Li-S cells, in order to maximize the endurance of the battery and fulfill the power requirements of the eVTOL. Additional weights are added to the nominal motor weight to take into account the gearboxes, housing, connections etc. An analytical framework based on the blade element and momentum theories is employed and modified to investigate different multirotor configurations and vertical flight conditions. With the last two models, three different configurations are designed starting from the helicopter layout. The models are compared on the basis of a typical mission made of an initial climbing phase, 2 min of hovering, a cruising phase, other 2 min of hovering and a descending phase. The different layouts have to fulfill a set of requirements related to the total weight, maximum size, payload and mission requirements (endurance and discharge limit). The results of the analysis showed that the helicopter is capable to complete the mission with an additional 2.3% of reserve and fulfills all the requirements set. This type of rotorcraft has the lowest power demand in hovering condition, but the higher level of profile power of the blades prevents you from reaching high speeds and climbing capabilities. The side – by – side and octarotor configurations are not able to complete the 50 min mission, although all the requirements are set to the limit values. These two configurations are very high-power demanding at low speed and a perfectly sized electrical motor is not available. As a consequence, the oversized motors provide too high available power with respect to the need of this mission. However, at least the side – by – side battery design allows to reach a discrete endurance of 40 min. The best configuration for the reference mission is the quadrotor: the reasonable power demand and the good sizing of the EMRAX motors make this layout the most suitable to complete the entire flight and add additional benefits to the vehicle.

In conclusion, the optimal configuration to complete the mission is identified in the quadrotor design and a reliable methodology to design electrical multirotor configurations is presented. Additional refinements to the model can be added by performing experimental tests and improving the numerical framework. In particular, an ad-hoc discharge model for Li-S batteries with high number of cells should be developed in order to better compute the endurance under a constant power loading. Additional components and efficiencies should be taken into account. For instance, the gearbox design has to allow variable rotational speed in the multirotor configurations, while a constant Ω and variable collective pitch system is used to control the helicopter. Actually, multirotors provide additional advantages in terms of maneuverability and simplicity of the systems which have not been taken into account in this analysis but play a fundamental role in lower-level design methodologies.

Appendix A

CONFIGURATION:			Helicopter
Motor type:			EMRAX 348 MV/CC
Symbol	**Value**	**Unit**	**Comments**
N_r	1	-	Number of main rotors
N_e	1	-	Number of motors
$MTOW$	588.39	kg	Maximum Take-off weight
m_0	184.11	kg	Empty mass: no payload, no battery, no motor. Include the blades.
m_p	175	kg	Payload
$MTOW_{max}$	600	kg	Maximum Take-Off Weight limit
f	0.2945	m^2	Equivalent flat plate drag area
f_{vert}	0.2945	m^2	Equivalent flat plate vertical drag area
P_s	0	W	Power of auxiliary systems
M_{dd}	0.74	-	Drag divergence drag
Main rotor:			
N_b	2	-	number of blades
R	3.8	m	radius
A	45.36	m^2	area
AR	19.49	-	aspect ratio
c	0.195	m	chord
DL	12.97	kg/m^2	disc loading
θ_l	-0.0367	rad/m	linear twist
σ	0.0327	-	solidity ratio
C_{d_0}	0.008	-	drag coefficient: $C_d = C_{d_0} + kC_l^2$
k	0.008	-	
Ω	55.34	rad/s	rotational frequency
VT	210.31	m/s	tip speed
η_{mr}	0.9	-	transmission efficiency
Tail rotor:			
N_{b_t}	2	-	number of blades
R_t	0.57	m	radius
A_t	1.021	m^2	area
c_t	0.12	m	chord
σ_t	0.0382	-	solidity ratio

Ω_t	320.63	rad/s	rotational frequency
VT_t	182.76	m/s	tip speed
$C_{d_0 t}$	0.008	-	drag coefficient: $C_d = C_{d_0} + kC_l^2$
k_t	0.008	-	
η_{tr}	0.9	-	transmission efficiency
l_{tr}	4.442	m	Distance between main and tail rotor centers

Table 7: Helicopter design

CONFIGURATION:			Side – by – side
Motor type:			EMRAX 268 MV/CC
Symbol	**Value**	**Unit**	**Comments**
N_r	2	-	Number of main rotors
N_e	2	-	Number of motors
$MTOW$	600	kg	Maximum Take-off weight
m_0	179.21	kg	Empty mass: no payload, no battery, no motor. Include the blades.
m_p	175	kg	Payload
$MTOW_{max}$	600	kg	Maximum Take-Off Weight limit
f	0.2945	m^2	Equivalent flat plate drag area
f_{vert}	0.2945	m^2	Equivalent flat plate vertical drag area
P_s	0	W	Power of auxiliary systems
M_{dd}	0.74	-	Drag divergence drag
Main rotor:			
N_b	3	-	number of blades
R	1.9	m	radius
A	11.34	m^2	area
AR	19.49	-	aspect ratio
c	0.0975	m	chord
DL	26.46	kg/m^2	disc loading
θ_l	-0.0367	rad/m	linear twist
σ	0.049	-	solidity ratio
C_{d_0}	0.008	-	drag coefficient: $C_d = C_{d_0} + kC_l^2$
k	0.008	-	
Ω	88.23	rad/s	rotational frequency
VT	167.64	m/s	tip speed

η_{mr}	0.9	-	transmission efficiency

Table 8: Side – by – side design

CONFIGURATION:			Quadrotor
Motor type:			EMRAX 208 MV/CC
Symbol	**Value**	**Unit**	**Comments**
N_r	4	-	Number of main rotors
N_e	4	-	Number of motors
$MTOW$	595.25	kg	Maximum Take-off weight
m_0	172.94	kg	Empty mass: no payload, no battery, no motor. Include the blades.
m_p	175	kg	Payload
$MTOW_{max}$	600	kg	Maximum Take-Off Weight limit
f	0.2945	m^2	Equivalent flat plate drag area
f_{vert}	0.2945	m^2	Equivalent flat plate vertical drag area
P_s	0	W	Power of auxiliary systems
M_{dd}	0.74	-	Drag divergence drag
Main rotor:			
N_b	2	-	number of blades
R	1.5	m	radius
A	7.07	m^2	area
AR	19.49	-	aspect ratio
c	0.077	m	chord
DL	21.05	kg/m^2	disc loading
θ_l	-0.0367	rad/m	linear twist
σ	0.0327	-	solidity ratio
C_{d_0}	0.008	-	drag coefficient: $C_d = C_{d_0} + kC_l^2$
k	0.008	-	
Ω	91.44	rad/s	rotational frequency
VT	137.16	m/s	tip speed
η_{mr}	0.9	-	transmission efficiency

Table 9: Quadrotor design

CONFIGURATION:			Octarotor
Motor type:			EMRAX 188 MV/CC
Symbol	**Value**	**Unit**	**Comments**
N_r	8	-	Number of main rotors
N_e	8	-	Number of motors
$MTOW$	598.42	kg	Maximum Take-off weight
m_0	173.57	kg	Empty mass: no payload, no battery, no motor. Include the blades.
m_p	175	kg	Payload
$MTOW_{max}$	600	kg	Maximum Take-Off Weight limit
f	0.2945	m²	Equivalent flat plate drag area
f_{vert}	0.2945	m²	Equivalent flat plate vertical drag area
P_s	0	W	Power of auxiliary systems
M_{dd}	0.74	-	Drag divergence drag
Main rotor:			
N_b	2	-	number of blades
R	0.95	m	radius
A	2.84	m²	area
AR	19.49	-	aspect ratio
c	0.0488	m	chord
DL	26.38	kg/m²	disc loading
θ_l	-0.0367	rad/m	linear twist
σ	0.0327	-	solidity ratio
C_{d_0}	0.008	-	drag coefficient: $C_d = C_{d_0} + kC_l^2$
k	0.008	-	
Ω	144.38	rad/s	rotational frequency
VT	137.16	m/s	tip speed
η_{mr}	0.9	-	transmission efficiency

Table 10: Octarotor design

REFERENCES

[1] B. P. Hill *et al.*, «UAM Vision Concept of Operations (ConOps) UAM Maturity Level (UML) 4», Grantee 20205011091, dic. 2020. [Online]. Disponibile su: https://ntrs.nasa.gov/citations/20205011091

[2] J. Zong, B. Zhu, Z. Hou, X. Yang, e J. Zhai, «Evaluation and Comparison of Hybrid Wing VTOL UAV with Four Different Electric Propulsion Systems», *Aerospace*, vol. 8, n. 9, 2021, doi: 10.3390/aerospace8090256.

[3] D. P. Thipphavong *et al.*, «Urban Air Mobility Airspace Integration Concepts and Considerations», presentato al AIAA AVIATION Forum, Atlanta, Georgia, giu. 2018. doi: 10.2514/6.2018-3676.

[4] W. Johnson, C. Silva, e E. Solis, «Concept Vehicles for VTOL Air Taxi Operations», presentato al AHS Technical Conference on Aeromechanics Design for Transformative Vertical Flight, San Francisco, CA, gen. 2018. [Online]. Disponibile su: https://ntrs.nasa.gov/citations/20180003381

[5] «CityAirbus NextGen - Urban Air Mobility - Airbus», 24 giugno 2021. https://www.airbus.com/en/innovation/zero-emission/urban-air-mobility/cityairbus-nextgen (consultato 18 luglio 2022).

[6] «Joby Aviation | Joby». https://www.jobyaviation.com/ (consultato 18 luglio 2022).

[7] A. Bacchini e E. Cestino, «Electric VTOL Configurations Comparison», *Aerospace*, vol. 6, n. 3, 2019, doi: 10.3390/aerospace6030026.

[8] «EHang | UAM - Passenger Autonomous Aerial Vehicle (AAV)». https://www.ehang.com/ehangaav/ (consultato 18 luglio 2022).

[9] «Lilium Jet - The First Electric VTOL (eVTOL) Jet - Lilium». https://lilium.com/jet (consultato 18 luglio 2022).

[10] G. Avanzini, E. L. de Angelis, e F. Giulietti, «Optimal cruise performance of a conventional helicopter», *Proc. Inst. Mech. Eng. Part G J. Aerosp. Eng.*, vol. 236, n. 5, pagg. 865–878, 2022, doi: 10.1177/09544100211024091.

[11] W. Johnson, *Helicopter Theory*. Courier Corporation, 2012.

[12] M. R. A. Nabawy e W. J. Crowther, «On the quasi-steady aerodynamics of normal hovering flight part I: the induced power factor», *J. R. Soc. Interface*, vol. 11, n. 93, pag. 20131196, 2014, doi: 10.1098/rsif.2013.1196.

[13] M. R. A. Nabawy e W. J. Crowther, «On the quasi-steady aerodynamics of normal hovering flight part II: model implementation and evaluation», *J. R. Soc. Interface*, vol. 11, n. 94, pag. 20131197, 2014, doi: 10.1098/rsif.2013.1197.

[14] A. R. Kadhiresan e M. J. Duffy, «Conceptual Design and Mission Analysis for eVTOL Urban Air Mobility Flight Vehicle Configurations», in *AIAA Aviation 2019 Forum*, American Institute of Aeronautics and Astronautics. doi: 10.2514/6.2019-2873.

[15] G. J. Leishman, *Principles of helicopter aerodynamics*. Cambridge university press, 2006. [Online]. Disponibile su: https://books.google.it/books?id=-PnV2JuLZi4C

[16] «Oxis Energy - Next Generation Battery Technology - Li2S», *Oxis Energy*. https://oxisenergy.com/ (consultato 18 luglio 2022).

[17] «EMRAX | Axial flux e-motors | lightweight | powerful», *EMRAX*. https://emrax.com/ (consultato 18 luglio 2022).

[18] G. Avanzini, E. L. de Angelis, e F. Giulietti, «Optimal performance and sizing of a battery-powered aircraft», *Aerosp. Sci. Technol.*, vol. 59, pagg. 132–144, 2016, doi: https://doi.org/10.1016/j.ast.2016.10.015.